**Eidgenössische Technische Hochschule Zürich**

*Ecole polytechnique fédérale de Zurich*
*Politecnico federale di Zurigo*
*Swiss Federal Institute of Technology Zurich*

# Entropy conservative and entropy stable finite volume schemes for multi-dimensional conservation laws on unstructured meshes

A. Madrane, U.S. Fjordholm, S. Mishra and E. Tadmor

Research Report No. 2012-31
October 2012

Seminar für Angewandte Mathematik
Eidgenössische Technische Hochschule
CH-8092 Zürich
Switzerland

# ENTROPY CONSERVATIVE AND ENTROPY STABLE FINITE VOLUME SCHEMES FOR MULTI-DIMENSIONAL CONSERVATION LAWS ON UNSTRUCTURED MESHES

AZIZ MADRANE, ULRIK S. FJORDHOLM, SIDDHARTHA MISHRA, AND EITAN TADMOR

ABSTRACT. We present entropy stable schemes for the two-dimensional Euler equations on unstructured grids. We develop a novel energy conservative scheme that is very simple to implement, is computationally cheap and is stable compared to other existing energy conservative schemes. To allow for a correct dissipation of energy in the vicinity of shocks, a novel numerical diffusion operator of the Roe type is designed. The energy conservative scheme, together with this diffusion operator, gives an energy stable scheme for Euler equation on unstructured grids. Numerical experiments are presented to demonstrate the robustness of the proposed schemes. Numerical experiments include the Sod shock tube problem, vortex advection and flow past a NACA0012 airfoil.

## 1. INTRODUCTION

We deal with systems of conservation laws in several space dimensions. For simplicity of exposition, we consider the two-dimensional case in this paper. The generic form of systems of conservation laws in two space dimensions is

$$\mathbf{U}_t + \mathbf{f}_1(\mathbf{U})_x + \mathbf{f}_2(\mathbf{U})_y = 0 \tag{1.1}$$

with $\mathbf{U} : \Omega \times \mathbb{R}_+ \to \mathbb{R}^m$ for some $\Omega \subset \mathbb{R}^2$. Defining $\mathbf{f}(\mathbf{U}) = (\mathbf{f}_1(\mathbf{U}),\ \mathbf{f}_2(\mathbf{U}))$, we say that (1.1) is *hyperbolic* if the matrix $\frac{d}{d\mathbf{U}}(\mathbf{f}(\mathbf{U}) \cdot \mathbf{n})$ has $m$ real eigenvalues for all nonzero $\mathbf{n} \in \mathbb{R}^2$. A prototypical example for (1.1) are the Euler equations of gas dynamics:

(1.2)
$$\mathbf{U} = \begin{pmatrix} \rho \\ \rho u \\ \rho v \\ \rho E \end{pmatrix}, \qquad \mathbf{f}_1(\mathbf{U}) = \begin{pmatrix} \rho u \\ \rho u^2 + p \\ \rho uv \\ (\rho E + p)u \end{pmatrix}, \qquad \mathbf{f}_2(\mathbf{U}) = \begin{pmatrix} \rho v \\ \rho uv \\ \rho v^2 + p \\ (\rho E + p)v \end{pmatrix}.$$

Here $m = \rho u,\ n = \rho v$ and $l = \rho E$, Let $\rho, u, v, p, E, c$ and $M$ denote the density, velocity components, pressure, total energy, speed of sound and Mach number. For a perfect gas the pressure the speed of sound and the Mach number are given by

$$p = (\gamma - 1)(\rho E - \frac{1}{2}\rho(u^2 + v^2)), \quad c = \sqrt{\frac{\gamma p}{\rho}}, \quad M = \frac{\sqrt{u^2 + v^2}}{c}. \tag{1.3}$$

We denote $\mathbf{u} = (u,\ v)$.

*Date*: May 11, 2012.
1991 *Mathematics Subject Classification.* 65M06,35L65.

1.1. **Entropy framework.** The solutions of (1.1) may develop discontinuities in finite time when even the initial data is smooth. Hence, solutions of (1.1) are sought in the sense of distributions. Additional admissibility criteria need to be imposed to single out unique solutions. Such criteria, called *entropy conditions*, rely on the existence of a convex function $\eta$ and functions $q_1, q_2$ such that the following compatibility conditions hold:

$$q_1'(\mathbf{U})^\top = \eta'(\mathbf{U})^\top \mathbf{f}_1'(\mathbf{U}), \qquad q_2'(\mathbf{U})^\top = \eta'(\mathbf{U})^\top \mathbf{f}_2'(\mathbf{U}). \tag{1.4}$$

It is straightforward to check using (1.4) that *smooth* solutions of (1.1) satisfy an additional conservation, the entropy identity

$$\eta(\mathbf{U})_t + q_1(\mathbf{U})_x + q_2(\mathbf{U})_y = 0. \tag{1.5}$$

However, entropy needs to be dissipated at shocks. Hence, the entropy identity (1.5) is replaced by an entropy inequality,

$$\eta(\mathbf{U})_t + q_1(\mathbf{U})_x + q_2(\mathbf{U})_y \leq 0, \tag{1.6}$$

that holds in the sense of distributions. The vector $\mathbf{V} = \eta'(\mathbf{U})$ is termed as the vector of *entropy variables*. The entropy inequality (1.6) is integrated in space to yield the stability estimate

$$\frac{d}{dt}\int_{\mathbb{R}^2} \eta(\mathbf{U}(x,y,t))dxdy \leq 0. \tag{1.7}$$

Thus, the entropy framework provides an a priori stability estimate for the mult-dimensional system (1.1).

We illustrate the entropy framework for the Euler equations (1.2). Define the standard logarithmic entropy $s := \log(p) - \gamma\log(\rho)$. Then the entropy function and entropy fluxes for the Euler equations are given by

$$\eta(\mathbf{U}) = -\frac{\rho s}{\gamma - 1}, \quad q_1(\mathbf{U}) = -\frac{\rho u s}{\gamma - 1}, \quad q_2(\mathbf{U}) = -\frac{\rho v s}{\gamma - 1}. \tag{1.8}$$

The entropy variables are

$$\mathbf{V} = \left(\frac{\gamma - s}{\gamma - 1} - \frac{\rho|\mathbf{u}|^2}{p},\ \frac{\rho u}{p},\ \frac{\rho v}{p},\ -\frac{\rho}{p}\right)^\top. \tag{1.9}$$

1.1.1. *Symmetrization:* The results of Godunov and Mock show that a hyperbolic system (1.1) is symmetrizable if and only if it has an entropy framework. A particularly revealing form of this symmetrization is due to Barth [1]. The key to this symmetrized form is a theorem of [1] showing that for every nonzero $\mathbf{n} \in \mathbb{R}^2$, there exist suitably scaled matrix of eigenvectors $R_{\mathbf{n}}$ of the matrix $\frac{d}{d\mathbf{U}}(\mathbf{f}(\mathbf{U})\cdot\mathbf{n})$ such that

$$R_{\mathbf{n}} R_{\mathbf{n}}^\top = \mathbf{U}_{\mathbf{V}}, \tag{1.10}$$

with $\mathbf{U}_{\mathbf{V}} = \mathbf{U}'(\mathbf{V})$ being the change-of-variables matrix from the conserved variables $\mathbf{U}$ to the entropy variables $\mathbf{V}$. This identity is independent of the direction $\mathbf{n}$, thus providing a natural scaling for the eigenvectors. Denote $R_k = R_{\mathbf{e}_k}$, with $\mathbf{e}_k$ being the unit vector in direction $k$, and let $\Lambda_k$ be the corresponding diagonal matrix of eigenvalues. Using (1.10), we obtain

$$\begin{aligned}
\mathbf{U}_t + \mathbf{f}_1(\mathbf{U})_x + \mathbf{f}_2(\mathbf{U})_y &= \mathbf{U}_t + \mathbf{f}_1'(\mathbf{U})\mathbf{U}_x + \mathbf{f}_2'(\mathbf{U})\mathbf{U}_y, \\
&= \mathbf{U}_{\mathbf{V}}\mathbf{V}_t + R_1\Lambda_1 R_1^{-1}\mathbf{U}_{\mathbf{V}}\mathbf{V}_x + R_2\Lambda_2 R_2^{-1}\mathbf{U}_{\mathbf{V}}\mathbf{V}_y, \\
&= \mathbf{U}_{\mathbf{V}}\mathbf{V}_t + R_1\Lambda_1 R_1^{\top}\mathbf{V}_x + R_2\Lambda_2 R_2^{\top}\mathbf{V}_y.
\end{aligned}$$

As $\eta$ is a convex function, $\mathbf{U_V}$ is a symmetric positive definite matrix. Clearly the coefficient matrices $R_k\Lambda_k R_k^\top$ for $k = 1, 2$ are symmetric, implying that the conservation law (1.1) has the symmetrized form

$$\mathbf{U_V}\mathbf{V}_t + R_1\Lambda_1 R_1^\top \mathbf{V}_x + R_2\Lambda_2 R_2^\top \mathbf{V}_y = 0. \tag{1.11}$$

For the Euler equations with the aforementioned entropy function, the change of variables matrix is given by

$$\mathbf{U_V} = \begin{pmatrix} \rho & \rho\mathbf{u}^\top & E \\ \rho\mathbf{u} & \rho\mathbf{u}\mathbf{u}^\top + p\mathbf{I} & \rho H\mathbf{u} \\ E & \rho H\mathbf{u}^\top & \rho H^2 - \frac{c^2 p}{\gamma - 1} \end{pmatrix}$$

where the specific enthalpy is $H = \frac{c^2}{\gamma-1} + \frac{|\mathbf{u}|^2}{2}$. The resulting scaled eigenvectors are

$$\begin{aligned} r^1_{\mathbf{n}} &= \sqrt{\frac{\rho(\gamma-1)}{\gamma}} \left( n_1,\ un_1,\ vn_1,\ \frac{(u^2+v^2)n_1}{2} \right)^\top, \\ r^2_{\mathbf{n}} &= \sqrt{\frac{\rho(\gamma-1)}{\gamma}} \left( 0,\ -\frac{cn_2}{\sqrt{\gamma-1}},\ \frac{cn_1}{\sqrt{\gamma-1}},\ -\frac{(vn_1 - un_2)c}{\sqrt{\gamma-1}} \right)^\top, \\ r^3_{\mathbf{n}} &= \sqrt{\frac{\rho}{2\gamma}} \left( 1,\ u + cn_1,\ v + cn_2,\ H + c(un_1 + vn_2) \right)^\top, \\ r^4_{\mathbf{n}} &= \sqrt{\frac{\rho}{2\gamma}} \left( 1,\ u - cn_1,\ v - cn_2,\ H - c(un_1 + vn_2) \right)^\top. \end{aligned} \tag{1.12}$$

The diagonal matrix of eigenvalues is given by

$$\Lambda_{\mathbf{n}} = \operatorname{diag}\big(un_1 + vn_2,\ un_1 + vn_2,\ un_1 + vn_2 + c,\ un_1 + vn_2 - c\big). \tag{1.13}$$

## 2. Discretization

2.1. **Mesh description.** We assume that $\Omega$ is a bounded polyhedral domain of $\mathbb{R}^2$. We introduce a conforming triangulation $\mathcal{T}_h$ in $\mathbb{R}^2$, where $h$ is the maximal length of the edges in $\mathcal{T}_h$. For the primary grid (see Figure 1(a)), the nodes are the vertices $a_i$, indexed over $i \in \mathcal{V}$, of the triangles $K \in \mathcal{T}_h$. The finite volume cells are the barycentric cells $C_i$, obtained by joining the midpoints $M_{ij}$ of the sides originating at node $a_i$ to the centroids $G_{ij}$ of the triangles of $\mathcal{T}_h$ which meet at $a_i$ (see Figure 1(b)). In the sequel we use the following notation.

**Notation 2.1.** Let $a_i, a_j, a_k$ be the three nodes defining a triangle $K \in \mathcal{T}_h$. Then

- $a_i$ is the $i^{\text{th}}$ vertex
- $M_{ij}$ is the midpoint of side $a_ia_j$
- $\mathcal{N}_i$ is the set of vertices that are neighbors of node $a_i$
- $|\mathcal{N}_i|$ is the number of neighboring vertices to $a_i$
- $G_{ij}$ $(j = 1, \ldots, |\mathcal{N}_i|)$ is the centroid of a triangle of which $a_i$ is a vertex
- $C_i$ is the barycentric cell constructed around $a_i$
- $e_{ij} = \partial C_i \cap \partial C_j$ is the common face of neighboring cells $C_i$ and $C_j$
- $\mathbf{n}_i = (n_{i_x}, n_{i_y})$ is the outward normal vector to $\partial C_i$
- $\mathbf{n}^1_{ij}, \mathbf{n}^2_{ij}$ are the normals of the two components of $e_{ij}$ (see Figure 2(a))
- $\mathbf{U}^n_i \cong \mathbf{U}(a_i, t^n)$ is the nodal cell average values at time $t = t^n$.

The union of all the barycentric cells constitutes a partition of the computational domain $\Omega_h$:

$$\Omega_h = \bigcup_{i=1}^{\mathrm{nv}} C_i$$

where nv is the number of vertices of the original finite element triangulation $\mathcal{T}_h$. For complete details of the domain of computation for the NACA0012 airfoil in the 2D see Figure 3.

Let

$$\mathbf{n}_{ij} = \int_{\partial C_i \cap \partial C_j} \mathbf{n}\, d\sigma = \mathbf{n}_{ij}^1 + \mathbf{n}_{ij}^2$$

be the unit normal on the face $e_{ij} = G_{ij}G_{i,j+1}$ pointing out of the control volume $C_i$. The normal vectors $\mathbf{n}_{ij}^1$ and $\mathbf{n}_{ij}^2$ are depicted in Figure 2(a) and $\mathbf{n}_{ij}$ in Figure 2(b). Note that we have

$$\sum_{j \in \mathcal{N}_i} \mathbf{n}_{ij} = 0. \tag{2.1}$$

We denote the average and difference of $\mathbf{U}$ across the edge $e_{ij}$ as

$$\overline{\mathbf{U}}_{ij} := \frac{1}{2}\left(\mathbf{U}_i + \mathbf{U}_j\right), \qquad [\![\mathbf{U}]\!]_{ij} := \mathbf{U}_j - \mathbf{U}_i,$$

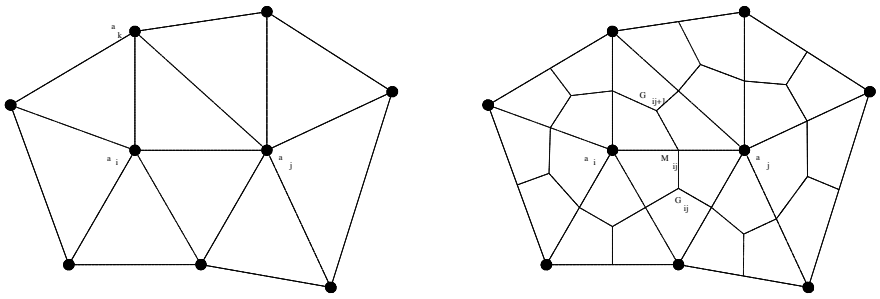

(a) Primary grid

(b) Barycentric cells around nodes $\boldsymbol{a_i}, \boldsymbol{a_j}$

FIGURE 1. Primary and dual grid

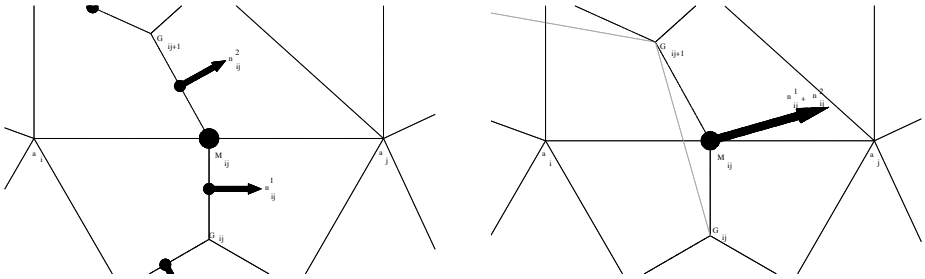

(a) Part of a boundary of $C_i$, $e_{ij} = \partial C_i \cap \partial C_j$ and the normal vectors $\mathbf{n}_{ij}^1$ and $\mathbf{n}_{ij}^2$

(b) Part of a boundary of $C_i$, $e_{ij} = \partial C_i \cap \partial C_j$ and the normal vector $\mathbf{n}_{ij}$

FIGURE 2. Triangle boundary and normals

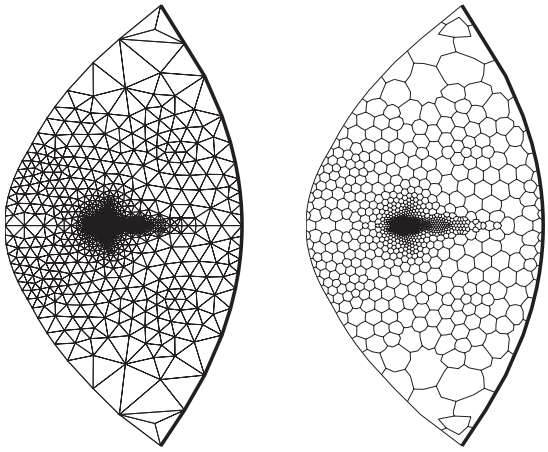

FIGURE 3. NACA0012 airfoil, Primary grid and barycentric cell $C_i$

and remark that $\overline{\mathbf{U}}_{ij} = \overline{\mathbf{U}}_{ji}$ and $[\![\mathbf{U}]\!]_{ij} = -[\![\mathbf{U}]\!]_{ji}$.

2.2. **Semi-discrete finite volume scheme:** The space discretization method considered here is a vertex centered finite volume formulation. In order to set the appropriate frame for the discrete problem which will be solved to approximate the solution of the original problem, we introduce the following **discrete spaces** (IS THIS NECESSARY?)

$$\mathcal{V}_h = \{v_h | v_h \in L^2(\Omega), v_h|_{C_i} = v_i = \text{const}; \;\; i = 1, \cdots, nv\} \tag{2.2}$$

A conservative and consistant finite volume approximation of (1.1) is written

$$\frac{\partial \mathbf{U}_h}{\partial t} + \frac{1}{|C_i|} \sum_{j \in K(i)} \mathbf{F}(\mathbf{U}_i, \mathbf{U}_j, \mathbf{n}_{ij}) = 0. \tag{2.3}$$

The numerical flux $\mathbf{F}_{ij} = \mathbf{F}(\mathbf{U}_i, \mathbf{U}_j, \mathbf{n}_{ij})$ is assumed to have the following properties:

(i) **Consistency:**

$$\mathbf{F}(\mathbf{U}, \mathbf{U}, \mathbf{n}) = \mathbf{f}(\mathbf{U}) \cdot \mathbf{n}$$

(ii) **Conservation:**

$$\mathbf{F}_{ij} = -\mathbf{F}_{ji}$$

for all $j \in \mathcal{N}_i$.

## 3. Entropy conservative schemes

We aim to design a numerical flux such that the resulting numerical scheme (2.3) is *entropy conservative* i.e, it satisfies a discrete version of the entropy identity (1.5). The concept of entropy conservative schemes for systems of conservation laws was introduced by Tadmor in [8] for Cartesian meshes. In this section we extend the notion of entropy conservative schemes to unstructured meshes.

**Definition 3.1.** A numerical flux $\widetilde{\mathbf{F}}_{ij} = \mathbf{F}(\mathbf{U}_i, \mathbf{U}_j, \mathbf{n}_{ij})$ is *entropy conservative* if it is of the form $\widetilde{\mathbf{F}}_{ij} = \widetilde{\mathbf{F}}^1_{ij} n^1_{ij} + \widetilde{\mathbf{F}}^2_{ij} n^2_{ij}$ and the components satisfy the relations

$$[\![\mathbf{V}]\!]^\top_{ij} \widetilde{\mathbf{F}}^k_{ij} = [\![\psi^k]\!]_{ij} \qquad k = 1, 2, \tag{3.1}$$

where $\psi_k(\mathbf{U}) = \mathbf{V}(\mathbf{U})^\top \mathbf{f}_k(\mathbf{U}) - q_k(\mathbf{U})$ denotes the entropy potential.

**Theorem 3.2.** *Let $\widetilde{\mathbf{F}}$ be an entropy conservative flux. Then the approximate solutions $\mathbf{U}_i$ computed by the finite volume scheme* (2.3) *with numerical flux $\widetilde{\mathbf{F}}$ satisfies the discrete entropy identity*

$$\frac{d}{dt}\eta(\mathbf{U}_i) + \frac{1}{|C_i|} \sum_{j \in \mathcal{N}_i} \widetilde{Q}_{ij} = 0 \tag{3.2}$$

*with numerical entropy flux*

$$\widetilde{Q}_{ij} := \sum_{k=1}^{2} n^k_{ij} \left( \overline{\mathbf{V}}^\top_{ij} \widetilde{\mathbf{F}}^k_{ij} - \overline{\psi^k}_{ij} \right). \tag{3.3}$$

*Proof.* Multiplying (2.3) by the entropy variables $\mathbf{V}_i$, we get

$$\begin{aligned}
\frac{d}{dt}\eta(\mathbf{U}_i) &= - \sum_{j \in \mathcal{N}_i} \frac{1}{|C_i|} \sum_{k=1}^{2} n^k_{ij} \mathbf{V}_i^\top \widetilde{\mathbf{F}}^k_{ij} \\
&= - \sum_{j \in \mathcal{N}_i} \frac{1}{|C_i|} \sum_{k=1}^{2} n^k_{ij} \left( \overline{\mathbf{V}}^\top_{ij} \widetilde{\mathbf{F}}^k_{ij} - \frac{1}{2} [\![\mathbf{V}]\!]^\top_{ij} \widetilde{\mathbf{F}}^k_{ij} \right) \\
&= - \sum_{j \in \mathcal{N}_i} \frac{1}{|C_i|} \sum_{k=1}^{2} n^k_{ij} \left( \overline{\mathbf{V}}^\top_{ij} \widetilde{\mathbf{F}}^k_{ij} - \frac{1}{2} [\![\psi^k]\!]_{ij} \right) \\
&= - \sum_{j \in \mathcal{N}_i} \frac{1}{|C_i|} \sum_{k=1}^{2} n^k_{ij} \left( \overline{\mathbf{V}}^\top_{ij} \widetilde{\mathbf{F}}^k_{ij} - \overline{\psi^k}_{ij} \right),
\end{aligned}$$

where we have used the identity (2.1) and added $\sum_{j \in \mathcal{N}_i} \sum_{k=1}^{2} \frac{1}{|C_i|} n^k_{ij} \psi^k_i = 0$. □

We note that the condition (3.1) provides a single algebraic equation for $m$ unknowns. In general, it is not clear whether a solution of (3.1) exists. Furthermore, the solutions of (3.1) will not be unique except for scalar equations. In [8], Tadmor showed the existence of at least one solution of (3.1) for any system of conservation laws. Explicit solutions were constructed in [9]. However, the entropy conservative fluxes of [9] are computationally expensive; see [2]. Instead, we follow recent papers [2, 7] to obtain algebraically simple and computational inexpensive solution of (3.1). For concreteness we consider the Euler equations of gas dynamics (1.2).

Denote by $Z$ the so-called Roe parameter vector

$$Z = \sqrt{\frac{\rho}{p}} \begin{pmatrix} 1 \\ u \\ v \\ p \end{pmatrix}.$$

It is readily verified that

$$\rho = Z_1 Z_4, \quad p = \frac{Z_4}{Z_1}, \quad u = \frac{Z_2}{Z_1}, \quad v = \frac{Z_3}{Z_1}, \quad m_1 = \rho u = Z_2 Z_4, \quad m_2 = \rho v = Z_3 Z_4$$

Denoting by $s = \log(p) - \gamma \log(\rho)$ the standard logarithmic entropy, we have

$$s = \ln\left(\frac{Z_4^{(1-\gamma)}}{Z_1^{(1+\gamma)}}\right), \qquad \eta(\mathbf{U}) = \frac{-Z_1 Z_4 s}{\gamma - 1}.$$

The entropy variables are

$$\mathbf{V} = \begin{pmatrix} \frac{\gamma - S}{\gamma - 1} - \frac{m_1^2 + m_2^2}{2p\rho} \\ \frac{m_1}{p} \\ \frac{m_2}{p} \\ -\frac{\rho}{p} \end{pmatrix} = \begin{pmatrix} \frac{\gamma}{\gamma-1} + \ln(Z_4) + (\frac{1+\gamma}{1-\gamma}) \ln Z_1 - \frac{Z_2^2 + Z_3^2}{2} \\ Z_1 Z_2 \\ Z_1 Z_3 \\ -Z_1^2 \end{pmatrix},$$

the entropy fluxes are

$$q_1(\mathbf{U}) = \frac{-m_1 S}{\gamma - 1} = \frac{-Z_2 Z_4 S}{\gamma - 1}, \qquad q_2(\mathbf{U}) = \frac{-m_2 S}{\gamma - 1} = \frac{-Z_3 Z_4 S}{\gamma - 1}$$

and the entropy potentials are

$$\psi_1(\mathbf{U}) = m_1, \qquad \psi_2(\mathbf{U}) = m_2.$$

Upon solving (3.1) we get the entropy conservative fluxes

$$\widetilde{\mathbf{F}}_1 = \begin{pmatrix} \widetilde{\mathbf{F}}_1^1 \\ \widetilde{\mathbf{F}}_1^2 \\ \widetilde{\mathbf{F}}_1^3 \\ \widetilde{\mathbf{F}}_1^4 \end{pmatrix} = \begin{pmatrix} \bar{Z}_2 Z_4^{\ln} \\ \frac{\bar{Z}_4 + \widetilde{F}^{1,1} \bar{Z}_2}{\bar{Z}_1} \\ \frac{\bar{Z}_2 \bar{Z}_3 Z_2^{\ln}}{\bar{Z}_1} \\ \frac{\frac{\gamma+1}{\gamma-1} \frac{1}{Z_1^{\ln}} \widetilde{F}_1^1 + \bar{Z}_2 \widetilde{F}_1^2 + \bar{Z}_3 \widetilde{F}_1^3}{2\bar{Z}_1} \end{pmatrix}$$

and

$$\widetilde{\mathbf{F}}_2 = \begin{pmatrix} \widetilde{\mathbf{F}}_2^1 \\ \widetilde{\mathbf{F}}_2^2 \\ \widetilde{\mathbf{F}}_2^3 \\ \widetilde{\mathbf{F}}_2^4 \end{pmatrix} = \begin{pmatrix} \bar{Z}_3 Z_4^{\ln} \\ \frac{\bar{Z}_2 \widetilde{F}_2^1}{\bar{Z}_1} \\ \frac{\bar{Z}_4 + \widetilde{F}_2^1 \bar{Z}_3}{\bar{Z}_1} \\ \frac{\frac{\gamma+1}{\gamma-1} \frac{1}{Z_1^{\ln}} \widetilde{F}_2^1 + \bar{Z}_2 \widetilde{F}_2^2 + \bar{Z}_3 \widetilde{F}_2^3}{2\bar{Z}_1} \end{pmatrix}.$$

Here, $a^{\ln}$ is the logarithmic mean defined as

$$a^{\ln} = \frac{[\![a]\!]}{[\![\log(a)]\!]}$$

See [7] for further details.

## 4. Entropy stable schemes for Euler equations

4.1. **Numerical diffusion operators.** The entropy conservative schemes lead to unphysical oscillations near shocks. We need to add numerical diffusion to eliminate these oscillations. Following the procedure of [2], we consider numerical flux functions

$$\mathbf{F}_{ij} = \widetilde{\mathbf{F}}_{ij} - \frac{1}{2}\mathbf{D}_{ij}[\![\mathbf{V}]\!]_{ij}. \tag{4.1}$$

Here, $\widetilde{\mathbf{F}}$ is an entropy conservative flux and $\mathbf{D}$ is any symmetric positive definite matrix with $\mathbf{D}_{ij} = \mathbf{D}_{ji}$. The flux $\mathbf{F}_{ij}$ is consistent because $\mathbf{U}_i = \mathbf{U}_j$ implies that $\mathbf{F}_{ij} = \widetilde{\mathbf{F}}_{ij} - 0 = \mathbf{f}(\mathbf{U}_i) \cdot \mathbf{n}_{ij}$, and it is conservative because $\mathbf{F}_{ji} = \widetilde{\mathbf{F}}_{ji} - \frac{1}{2}\mathbf{D}_{ji}\left(-[\![\mathbf{V}]\!]_{ij}\right) = -\left(\widetilde{\mathbf{F}}_{ij} - \frac{1}{2}\mathbf{D}_{ij}[\![\mathbf{V}]\!]_{ij}\right) = -\mathbf{F}_{ij}$.

The scheme with numerical flux (4.1) is entropy stable by the following lemma.

**Lemma 4.1.** *Let the numerical flux in the finite volume scheme* (2.3) *be defined by* (4.1). *Then the approximate solutions* $\mathbf{U}_i$ *computed by the scheme* (2.3) *satisfy the discrete entropy inequality*

$$\frac{d}{dt}\eta(\mathbf{U}_i) + \sum_{j\in N_i} \frac{1}{|C_i|} Q_{ij} \leq 0, \tag{4.2}$$

*with numerical entropy flux* $Q$ *given by*

$$Q_{ij} = \widetilde{Q}_{ij} - \frac{1}{2}\overline{\mathbf{V}}_{ij}^{\top}\mathbf{D}_{ij}[\![\mathbf{V}]\!]_{ij},$$

*where* $\widetilde{Q}$ *is defined in* (3.3). *Summing over* $i \in \mathcal{V}$, *we obtain the entropy bound*

$$\frac{d}{dt}\sum_{i\in\mathcal{V}} \eta(\mathbf{U}_i) \leq 0. \tag{4.3}$$

*Proof.* Multiplying the finite volume formulation (2.3) by $\mathbf{V}_i$ we get

$$\begin{aligned}
\frac{d}{dt}\eta(\mathbf{U}_i) &= -\sum_{j\in\mathcal{N}_i} \frac{1}{|C_i|}\left(\mathbf{V}_i^{\top}\widetilde{\mathbf{F}}_{ij} - \frac{1}{2}\mathbf{V}_i^{\top}\mathbf{D}_{ij}[\![\mathbf{V}]\!]_{ij}\right) \\
&= -\sum_{j\in\mathcal{N}_i} \frac{1}{|C_i|}\left(\widetilde{Q}_{ij} - \frac{1}{2}\left(\overline{\mathbf{V}}_{ij}^{\top} - \frac{1}{2}[\![\mathbf{V}]\!]_{ij}^{\top}\right)\mathbf{D}_{ij}[\![\mathbf{V}]\!]_{ij}\right) \\
&= -\sum_{j\in\mathcal{N}_i} \frac{1}{|C_i|} Q_{ij} - \frac{1}{4}\sum_{j\in N_i}\frac{1}{|C_i|}[\![\mathbf{V}]\!]_{ij}^{\top}\mathbf{D}_{ij}[\![\mathbf{V}]\!]_{ij} \\
&\leq -\sum_{j\in\mathcal{N}_i} \frac{1}{|C_i|} Q_{ij},
\end{aligned}$$

thus proving (4.2). □

4.2. **Specifying the numerical diffusion matrix.** Following [2, 3], we choose the following numerical diffusion matrix:

$$\mathbf{D}_{ij} = R_{\mathbf{n}_{ij}}|\Lambda_{\mathbf{n}_{ij}}|R_{\mathbf{n}_{ij}}^{\top}. \tag{4.4}$$

Here, $\Lambda_{\mathbf{n}}$ and $R_{\mathbf{n}}$ are the matrix of eigenvalues and eigenvectors as defined in (1.10). The matrices can be evaluated at the average state $\overline{\mathbf{U}}_{ij}$.

## 5. Numerical experiments

5.1. **Vortex advection.** We start testing the scheme on a smooth test case for the two-dimensional Euler equations. This test case involves long time simulation. The initial data is set in terms of velocity $u$ and $v$, the temperature $\theta = \frac{p}{\rho}$ and entropy $s = \log p - \gamma \log \rho$:

$$u = 1 - (y - y_c)\varphi(r), \quad v = 1 - (x - x_c)\varphi(r), \quad \theta = 1 - \frac{\gamma - 1}{2\gamma}\varphi(r)^2$$

where $r = \sqrt{(x - x_c)^2 + (y - y_c)^2}$ with $(x_c, y_c)$ being the initial center of the vortex, and

$$\varphi(r) = \varepsilon e^{\alpha(1-\tau^2)}, \quad \tau = \frac{r}{r_c}$$

We set the free parameters, $\varepsilon = \frac{5}{2\pi}$, $\alpha = \frac{1}{2}$, $r_c = 1$ and $(x_c, y_c) = (5, 5)$. The exact solution of this initial value problem is simply $\mathbf{U}(x, y, t) = \mathbf{U}(x - t, y - t, 0)$. In other words, the initial vortex centered at $(x_c, y_c)$ is advected diagonally with a velocity of 1 in the $x$- and $y$-directions. The computational domain and initial

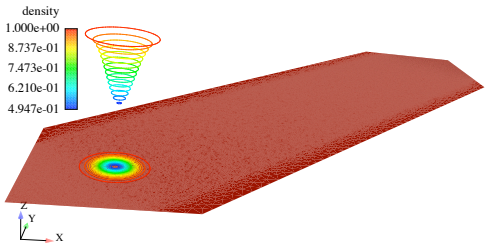


FIGURE 4. Computational domain with initial data, with slices in z-direction

data is shown in Figure 4. We compute up to $T = 30$ on a mesh with 40836 vertices. Figure 5 shows the computed density at the time $t = 30$ using the entropy conservative scheme and the Roe scheme. Figure 6 shows that there is a significant gain in accuracy using the entropy conservative scheme.

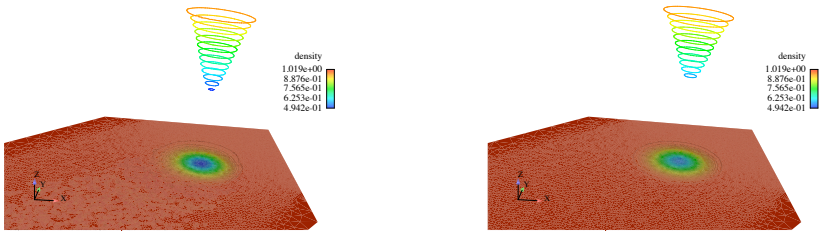


(a) Entropy conservative scheme (b) Roe scheme

FIGURE 5. $\rho$ at $t = 30$ with slices in z-direction.

5.2. **Sod shock tube in two dimensions.** We consider the Euler Equations in the computational domain $\Omega = [0, 1] \times [0, 0.1]$ with Riemann initial data

$$(\rho, m_1, m_2, l) = \begin{cases} (1, 0, 0, 2.5) & 0 < x < 0.5 \\ (0.125, 0, 0, 0.25) & 0.5 < x < 1. \end{cases}$$

The initial discontinuity breaks into a left-going rarefaction wave, a right-going shock and a right-going contact discontinuity. The computed solution at time $T = 1, 4$ (IS THIS SUPPOSED TO BE 1.4???) on a mesh of 20136 points, shown in Figure 7, has noticeable oscillations. On the other hand, the entropy stable scheme and the Roe scheme are quite good at resolving the waves; see Figure 8. The total entropy $\sum_{i \in \mathcal{V}} |C_i| \eta(\mathbf{U})_i$ versus time is shown in Figure 9.

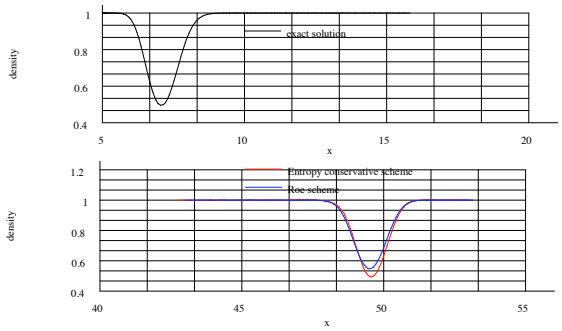


FIGURE 6. Entropy stable conservative scheme vs Roe scheme, $\rho$ at $t = 30$. Exact solution in red line.

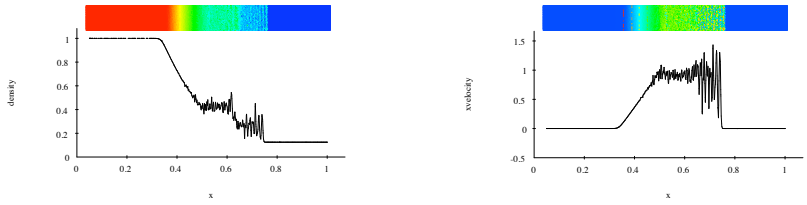


(a) Iso density (b) Iso velocity

FIGURE 7. Density and velocity FOR WHICH SCHEME?

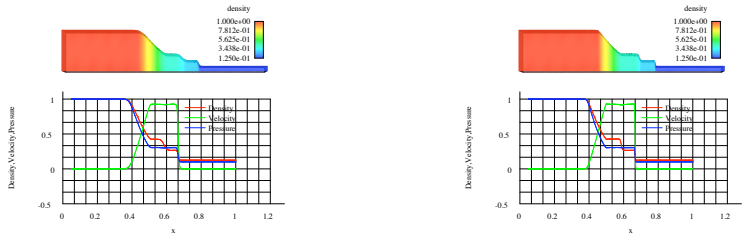


(a) Stable entropy conservative scheme (b) Roe scheme

FIGURE 8. CAPTION

5.3. **Simulation of transonic flows around a NACA 0012 airofoil.** We consider a transonic flow around a NACA0012 at angle of attack $\alpha = 1^o$ and Mach number at infinity $M_\infty = 0.85$. We have selected this problem since it is a quite classical and significant test problem for Euler solvers [5]. Figure 10 shows the final adapted triangulation near the profile used to solve the test problem. The mesh contains 14930 points. Figures 11(a), 11(b) show the pressure and density lines for the entropy stable scheme and Roe scheme. We can observe the similar shocks locations obtained with the two schemes implying a small difference in pressure distributions shown in Figure 12.

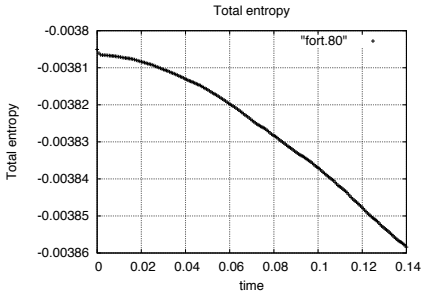


(a) entropy conservative scheme

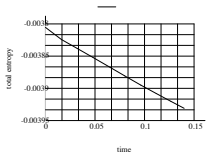

(b) Entropy stable conservative scheme

FIGURE 9. Total entropy vs. time

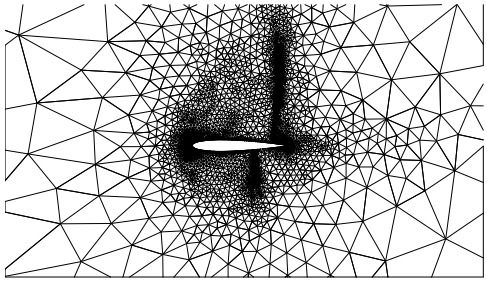

FIGURE 10. Adapted mesh

## 6. Conclusion

We have presented in this paper a new formulation of entropy stable conservative schemes on unstructured grids for the accurate numerical solution of Euler equations modelling transonic, supersonic and hypersonic flows. With these methods we can simulate 3-D flows around complex geometries such as complete space aircraft.

Variants of these methods can be extended to more complicated situations such as the coupling of two mathematical modellings using the Euler and Navier-Stokes equations.

## References

[1] T.J. BARTH, *Numerical methods for gaz-dynamics systems on unstructured meshes. In An introduction to Recent Developments in Theory and Numerics of Conservation Laws pp 195-285. Lecture Notes in Computational Science and Engineering Volume 5, Springer, Berlin. Eds D. Kroner, M. Ohlberger and Rohde, C., 1999*

[2] U.S. Fjordholm, S. Mishra and E. Tadmor, *Energy preserving and energy stable schemes for the shallow water equations. "Foundations of Computational Mathematics", Proc. FoCM held in Hong Kong 2008 (F. Cuckers, A. Pinkus and M. Todd, eds), London Math. Soc. Lecture Notes Ser. 363, pp. 93-139, 2009.*

[3] U.S. Fjordholm, S. Mishra and E. Tadmor, *Arbitrary high-order accurate entropy stable essentially non-oscillatory schemes for systems of conservation laws. In preparation, 2010.*

[4] S. Gottlieb, C.W. Shu, E. Tadmor, *High order time discretizations with strong stability proprties, SIAM. Review, 43 (2001), pp. 89-112.*

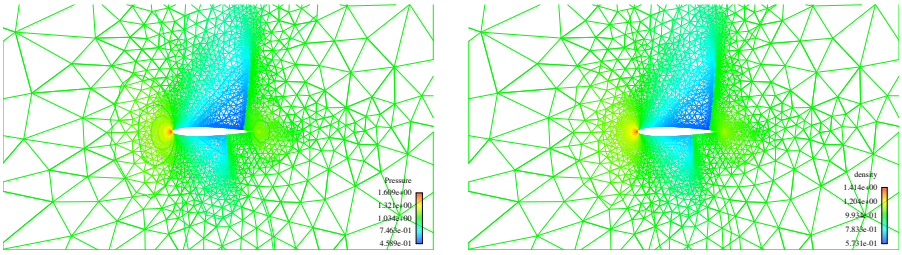

(a) ( entropy stable conservative scheme)

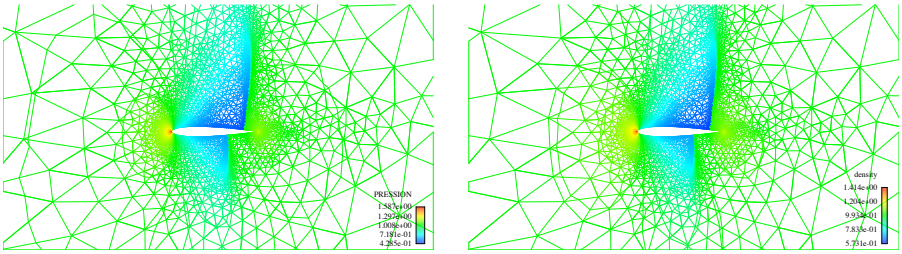

(b) (Roe scheme)

FIGURE 11. Iso-pressure and density lines

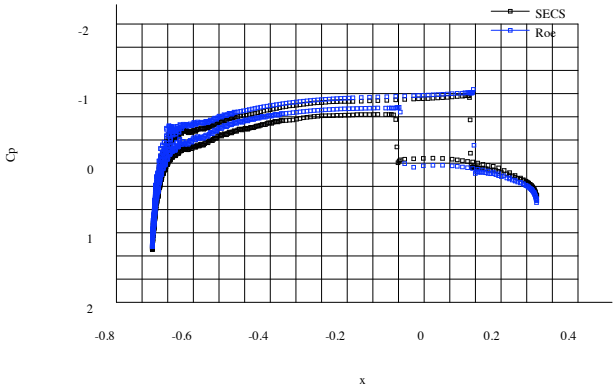


FIGURE 12. Pressure distribution (entropy stable conservative scheme vs. Roe scheme)

[5] GAMM WORKSHOP ON NUMERICAL SIMULATION OF COMPRESSIBLE EULER FLOWS, *France, 10-13 June 1986.*

[6] C. HIRSCH, *Numerical Computation of Internal and External Flows, Vol-2: Computational Methods for Inviscid and Viscous Flows, Wiley Series in Numerical Methods in Engineering, J. Wiley & Sons, 1990.*

[7] F. ISMAIL AND P. L. ROE, *Affordable, entropy-consistent Euler flux functions II: Entropy production at shocks. J. Comput. Phys., vol. 228, issue 15 (2009), pp. 5410–5436.*

[8] E. TADMOR, *The numerical viscosity of entropy stable schemes for systems of conservation laws*, I. Math. Comp., 49, 91-103, 1987.

[9] E. TADMOR, *Entropy stability theory for difference approximations of nonlinear conservation laws and related time–dependant problem*, Acta Numerica (2003), pp. 451–512.

(Aziz Madrane)
Bombardier Aerospace,
Montreal, Canada
*E-mail address*: aziz.madrane@aero.bombardier.com

(Ulrik S.Fjordholm)
Seminar for Applied Mathematics, ETH Zürich.
Rämistrasse 101, Zürich 8092, Switzerland
*E-mail address*: ulrikf@sam.math.ethz.ch

(Siddhartha Mishra)
Seminar for Applied Mathematics, ETH Zürich.
Rämistrasse 101, Zürich 8092, Switzerland
*E-mail address*: smishra@sam.math.ethz.ch

(Eitan Tadmor)
Department of Mathematics
Center of Scientific Computation and Mathematical Modeling (CSCAMM)
Institute for Physical sciences and Technology (IPST)
University of Maryland
MD 20742-4015, USA
*E-mail address*: tadmor@cscamm.umd.edu

# Research Reports

| No. | Authors/Title |
|---|---|
| 12-31 | *A. Madrane, U.S. Fjordholm, S. Mishra and E. Tadmor*<br>Entropy conservative and entropy stable finite volume schemes for multi-dimensional conservation laws on unstructured meshes |
| 12-30 | *G.M. Coclite, L. Di Ruvo, J. Ernest and S. Mishra*<br>Convergence of vanishing capillarity approximations for scalar conservation laws with discontinuous fluxes |
| 12-29 | *A. Abdulle, A. Barth and Ch. Schwab*<br>Multilevel Monte Carlo methods for stochastic elliptic multiscale PDEs |
| 12-28 | *E. Fonn, Ph. Grohs and R. Hiptmair*<br>Hyperbolic cross approximation for the spatially homogeneous Boltzmann equation |
| 12-27 | *P. Grohs*<br>Wolfowitz's theorem and consensus algorithms in Hadamard spaces |
| 12-26 | *H. Heumann and R. Hiptmair*<br>Stabilized Galerkin methods for magnetic advection |
| 12-25 | *F.Y. Kuo, Ch. Schwab and I.H. Sloan*<br>Multi-level quasi-Monte Carlo finite element methods for a class of elliptic partial differential equations with random coefficients |
| 12-24 | *St. Pauli, P. Arbenz and Ch. Schwab*<br>Intrinsic fault tolerance of multi level Monte Carlo methods |
| 12-23 | *V.H. Hoang, Ch. Schwab and A.M. Stuart*<br>Sparse MCMC gpc Finite Element Methods for Bayesian Inverse Problems |
| 12-22 | *A. Chkifa, A. Cohen and Ch. Schwab*<br>High-dimensional adaptive sparse polynomial interpolation and applications to parametric PDEs |
| 12-21 | *V. Nistor and Ch. Schwab*<br>High order Galerkin approximations for parametric second order elliptic partial differential equations |
| 12-20 | *X. Claeys, R. Hiptmair, and C. Jerez-Hanckes*<br>Multi-trace boundary integral equations |
| 12-19 | *Šukys, Ch. Schwab and S. Mishra*<br>Multi-level Monte Carlo finite difference and finite volume methods for stochastic linear hyperbolic systems |
| 12-18 | *Ch. Schwab*<br>QMC Galerkin discretization of parametric operator equations |